Beam shaping algorithm with optimization parameters

Nicolas Barré*

* Corresponding author: nicolas.barre83@gmail.com

March 15, 2022

Abstract

In this article, we present a general mode-conversion algorithm allowing to build an optical system composed of an alternation of phase masks and free propagations. The originality of our approach lies in the introduction of free parameters that can be used to perform an optimization regarding some properties of interest. Here, we apply this algorithm to overlap balancing, for the conversion of an important number of modes with limited phase resources. Moreover, we discuss about the convergence and the limitations of such an algorithm, notably concerning the loss of unitarity that tends to occur in a practical implementation.

1 Introduction

Beam shaping is a subject of great interest in the laser community since it is used in a broad range of applications, involving both low ang high power beams, such as micromanipulation [1], microscopy [2], optical communications in fibers or in free space [3], beam combining [4], or even material processing [5]. With the development of new techniques for realizing freeform optics [6], we can expect a further growth and spread of the interest for this field.

Beam shaping techniques can be classified in different categories, depending on whether they address monomode or multimode transformations, require single or multiple phase masks, or use a discrete or a continuous approach. On the one hand, a large range of applications only require monomode transformations, which are mostly achieved by shaping a Gaussian mode using a single phase mask [7]. In order to improve the conversion efficiency, multiple phase masks may be employed. Furthermore, we notice that beam shaping and phase retrieval problems are strongly linked, and computer generated holography is a rich domain from where many algorithms can be revisited [8]. The most famous iterative algorithm designed to perform phase retrieval on a single mode using two planes is the Gerchberg–Saxton algorithm [9]. This algorithm has then been extended to a larger number of planes [10], and even adapted recently to deal with a continuous medium [11], providing refractive index shaping for coherent beam combining or flat-top profile generation.

On the other hand, some applications are interested in multimode transformations which require even more phase resources. In [12], it has been shown theoretically that any unitary transformation can be achieved by a succession of phase masks separated by Fourier transforms. In their paper, the authors develop a stochastic approach in order to achieve up to 4–mode transformations. Very recently, a 45–mode conversion using a succession of phase masks separated by free propagations, based on a deterministic algorithm, has been presented in [13].

In this paper, we propose a general mode-conversion algorithm that extends the method [13] tackling several crucial points. Moreover, we introduce a proper formalization of the question of mode-conversion as an optimization problem, and derive an analytical expression for the optimal phase masks. In turn, this allows to perform some further optimizations, exploiting a set of free parameters. We show the potential of this general algorithm by applying it to one specific task, namely to the design of an optical system converting a large number of modes with balanced convergence rates, that could be used either as a beam combiner or as a spatial division multiplexer.

2 Mode-conversion algorithm

We present an algorithm designed to convert an orthogonal set of n modes $\{u_i\}_{1\leq i\leq n}$ defined in the input plane $z = z_{in}$, into a new orthogonal set of modes $\{v_i\}_{1\leq i\leq n}$ in the output plane $z = z_{out}$, by computing a set of k phase masks $\{\varphi_l\}_{1\leq l\leq k}$ located at positions z_l. The figure 1 illustrates such a configuration.

In the ideal case of infinitely thin and extended phase masks, the transformation performed by such a system is unitary, meaning that it conserves the scalar product in

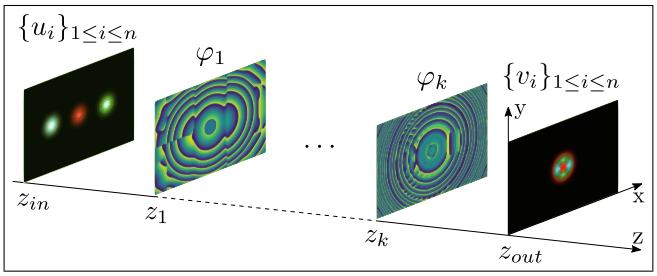

Fig. 1: Illustration of a n–mode transformation with k phase masks located at positions z_l, $1 \leq l \leq k$.

every transverse plane. Thus, we can define the overlaps o_i between the input and output modes by

$$\forall l,\ o_i = \int_{z=z_l} v_i^*(x,y,z_l) u_i(x,y,z_l) e^{\imath\varphi_l(x,y)} \mathrm{d}x\mathrm{d}y, \quad (1)$$

assuming that o_i does not depend on the plane $z = z_l$ where the integral (1) is computed. In order to know the modes u_i and v_i in the different planes, the former have to be propagated through the system whereas the latter need to be backpropagated.

Initially, the phase masks φ_l can be taken as constant or set to appropriate spherical phases in order to compensate for the divergence inside the system. The positions z_l can be chosen arbitrarily even though some positions may be better for the convergence of the algorithm. For instance, it is recommended that two consecutive planes are separated by a distance close to the average of u_i and v_i Rayleigh ranges, in order for diffraction to operate.

The algorithm consists in computing alternately each phase mask φ_l in order to maximize simultaneously all the o_i. The order of the masks calculation can be arbitrary and each mask may be computed multiple times until the algorithm reaches a fixed-point. Before computing the mask φ_l, the u_i and v_i have to be propagated (in the forward and backward direction respectively) to the plane $z = z_l$. Then, we define φ_l as the phase mask which maximizes the global overlap factor

$$\begin{aligned} O(\varphi) &= \Re\left(\sum_{i=1}^{n} \omega_i e^{\imath\theta_i} o_i\right) \quad (2)\\ &= \int_{z=z_l} \Re\Bigg(e^{\imath\varphi(x,y)} \times \\ &\qquad \sum_{i=1}^{n} \omega_i e^{\imath\theta_i} v_i^*(x,y,z_l) u_i(x,y,z_l)\Bigg) \mathrm{d}x\mathrm{d}y, \end{aligned}$$

where the $\omega_i \in \mathcal{R}^+$ and $\theta_i \in [0, 2\pi]$ are free parameters that are heuristically introduced in order to provide more flexibility to the algorithm. Indeed, the ω_i allow to adjust the relative weights of the modes in the transformation, while the θ_i are helpful when a constant relative phase between two modes does not matter. $O(\varphi)$ is real and when the u_i and v_i are normalized we have

$$0 \leq O(\varphi) \leq \sum_{i=1}^{n} \omega_i. \quad (3)$$

An interesting property of equation (2) is that the global maximization of $O(\varphi)$ reduces to local maximizations for x and y fixed, leading to an analytical expression for the optimal solution

$$\varphi_l(x,y) = -\arg\left(\sum_{i=1}^{n} \omega_i e^{\imath\theta_i} v_i^*(x,y,z_l) u_i(x,y,z_l)\right). \quad (4)$$

Then, the convergence of the algorithm relies on the monotone convergence theorem, which applies because $O(\varphi)$ is bounded, as already stated by (3), and always increasing. Indeed, each phase mask is computed in order to maximize O, and the unitarity of the system ensures that O is conserved in every plane.

Finally, it is interesting to notice that in the case of a one-mode transformation with two planes, when $z_{in} = z_1$ and $z_{out} = z_2$, the algorithm we describe is equivalent to the well known Gerchberg–Saxton (GS) algorithm [9]. In the historical formulation of the GS algorithm, the two distributions at planes z_1 and z_2 are supposed to be Fourier conjugated by a lens placed in between. However, this is not necessary to ensure the convergence of the algorithm; indeed any unitary transformation in between would work. Moreover, concerning the GS algorithm, it is known that the phase retrieval does not work optimally when the intensity distributions given initially present some measurement errors, or when the optical system placed in between is not rigorously modeled. In the same way, the algorithm we present will converge only partially if the provided phase resources are insufficient regarding the complexity of the unitary transformation to be performed.

3 Application to overlap balancing

Here, we propose to implement an optimization algorithm taking advantage of the free parameters ω_i introduced in (2), in order to provide the balancing of the overlaps o_i defined in (1). Thus, we introduce the optimization function

$$f(\{\omega_i\}) = \mathrm{Var}\left(|o_i|^2\right) - \alpha \mathrm{E}\left(|o_i|^2\right), \quad (5)$$

that we want to minimize. The dependance in ω_i of the right term of equation (5) comes from the dependance of

o_i in φ_l defined in (4). Equation (5) states that we intend to minimize the variance of the overlaps distribution while ensuring the mean overlap is kept to a high value. The constant $\alpha \in \mathcal{R}^{+*}$ is a tuning parameter allowing to give a similar scale to both terms of the equation. The choice of α is not so critical for the optimization to succeed.

There is no simple analytical expression to find the ω_i that minimize (5), which requires to use a numerical optimization technique working in a $(n-1)$–dimensional space, n being the number of modes. Indeed, equation (4) shows that the optimal phase masks remain invariant when the ω_i are multiplied by a global constant. This allows to always set $\omega_1 = 1$, for instance.

Equation (4) also introduces some phase parameters θ_i that still need to be defined. By inspection of equation (2), we see that an adequate choice is to set

$$\theta_i = -\arg\left(\int_{z=z_l} v_i^*(x,y,z_l)u_i(x,y,z_l)\mathrm{d}x\mathrm{d}y\right), \qquad (6)$$

$e^{\imath\theta_i}$ being the constant phase solution that maximizes the real part of o_i.

In [13], Fontaine et al. use an algorithm similar to what we described in section 2, but they do not introduce the free parameters ω_i, which is equivalent to choose all $\omega_i = 1$. In this paper, we aim to demonstrate the advantages of using an optimally weighted algorithm in comparison to an unparameterized algorithm ($\omega_i = 1$). In order to prove that the optimization of (5) scales with a significant number of modes, we propose to address a 45–mode transformation like in [13], which is described by figure 2.

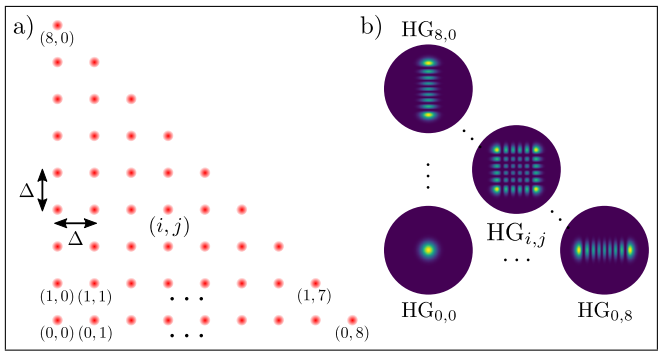

Fig. 2: a) Input mode layout : 45 Gaussians forming a triangle separated by a step Δ in each dimension. b) Mapping of input modes labelled (i, j) to co-propagating Hermite–Gaussian modes $\mathrm{HG}_{i,j}$.

According to [13], the conversion of Gaussian modes arranged in a triangle into co-propagating Hermite–Gaussian modes takes advantage of symmetries in order to reduce significantly the number of phase masks that would be needed otherwise. In their paper, they perform a simulation with 14 planes, some of them being dedicated to the adiabatic rearrangement of a linear array of gaussians into the required triangle layout. Here, we do not intend to reproduce this part that is not necessary for our purpose. Instead, we will limit the phase resources to 9 planes and deal directly with the mode-conversion problem presented in figure 2.

4 Results and discussion

For the simulation, we consider 9 planes separated by a constant distance $\Delta z = 24$ mm. The input Gaussian modes are defined in the first plane and have a waist of 70 μm. They are arranged in a triangle with a step $\Delta = 120$ μm. The output Hermite–Gaussian modes are defined at a distance Δz after the last plane and have a waist of 120 μm. The wavelength is set to $\lambda = 1.55$ μm and the simulation resolution in each transverse direction is defined by $\mathrm{d}x = \mathrm{d}y = 5$ μm, a transverse plane being represented as a grid of 512×724 pixels.

Free propagation plays a crucial role in the problem we intend to solve, and apart from the optimization of (5) it represents the most time-consuming part of the algorithm. A very efficient and standard method to propagate a field between two parallel planes is the angular spectrum method [14]. However, when using this method we notice that aliasing occurs from the first steps of the algorithm, coming from different origins. First, the natural divergence of the beams leads to energy folding on the edges of the grids, when the phase masks are not defined yet. Then, when applying equation (4) to compute the phase masks, some high spatial frequency invariably appear, thus increasing the beams divergence in some regions. A straightforward solution to prevent these effects is to limit the angular spectrum of plane waves, as already suggested in [13]. Thus, we decide to limit the maximum frequencies f_{xmax} and f_{ymax} in Fourier space by using a rectangular diaphragm, parameterized by a variable η leading to maximum frequencies f_{xmax}/η and f_{ymax}/η.

Now, in order to assess the performances of the algorithm, we need to define a mode-conversion efficiency. We achieve that through the squared overlaps $|o_i|^2$, representing the fraction of the energy of the input mode u_i that couples into the output mode v_i. To get a global information on the system performance, we also define a mean conversion efficiency by $\mathrm{E}(|o_i|^2)$. Furthermore, this will serve as a criterion for the convergence of the algorithm, instead of $O(\varphi)$ which is less physical.

The results of the simulation are collected in figure 3. First, figure 3a shows the incoherent sum of all mode

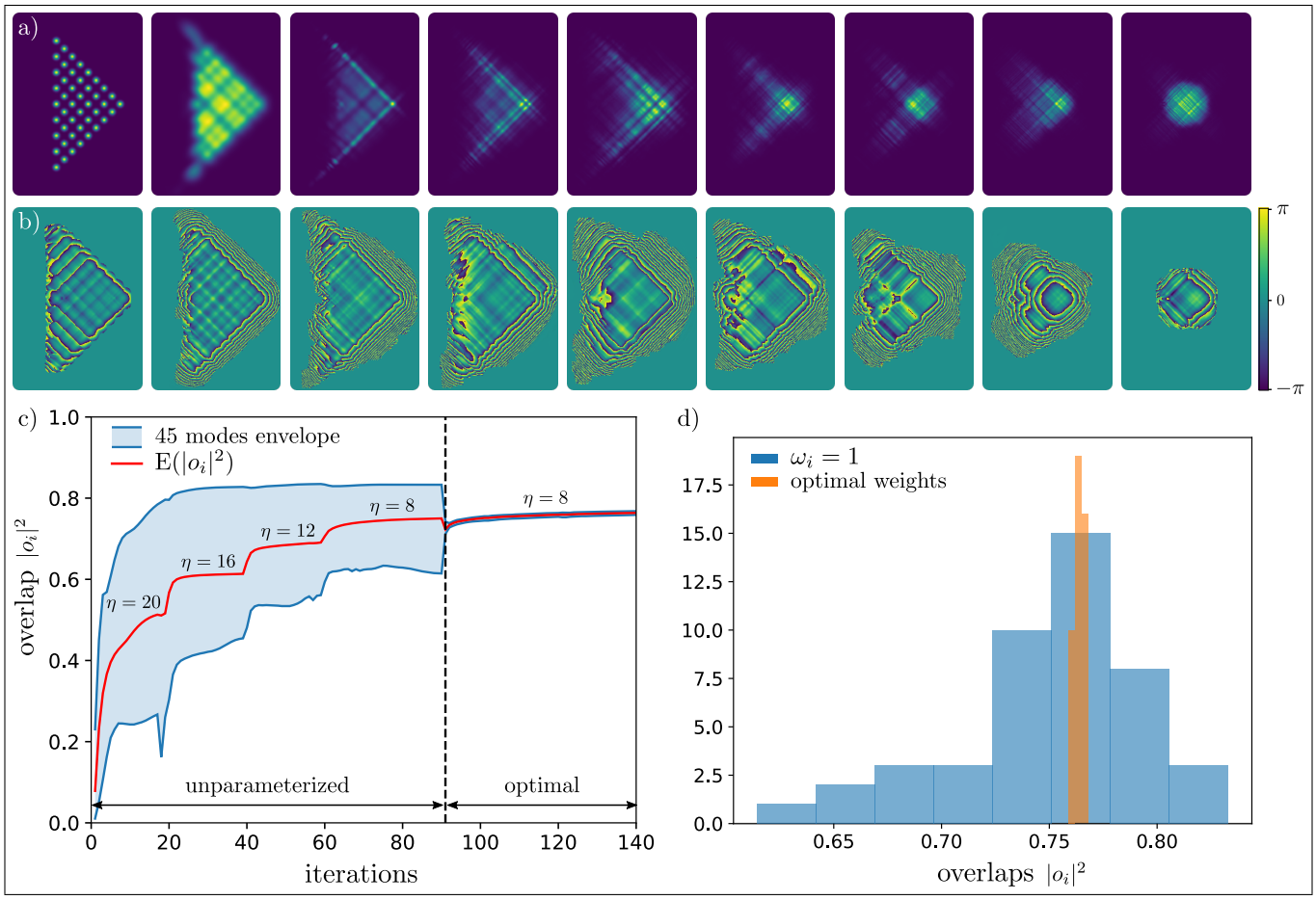

Fig. 3: Results of the simulation. a) Sum of all intensity profiles in each plane. b) Resulting phase masks performing the 45–mode transformation. c) Convergence of the mode overlaps, starting with 90 iterations of the unparameterized algorithm and ending with 50 iterations performing optimization. d) Histograms representing the distribution of overlaps among the 45 modes.

intensities in every plane, obtained with the optimally weighted algorithm. The input triangle is rotated by 135° counterclockwise compared to figure 2a. We observe that the separate Gaussian modes provided initially tend to form a more and more dense set of beams, until they get superimposed into a single beam composed mainly of co-propagating Hermite–Gaussian modes.

Then, figure 3b shows the phase masks that allow to perform this 45–mode conversion. All along the simulation, the phase masks have been cleared in regions representing less than 0.1% of the energy of the beams. This demonstrates that up to this limit there is no aliasing effect due to the edges of the grids. We notice that in regions of high energies the phase remains smooth and could be unwrapped with few if no discontinuities, whereas in other regions the phase starts to oscillate with fast spatial variations and is not necessarily continuous. We noticed that a stronger cleansing of the phase masks in order to get rid of these unwanted effects would reduce the final conversion efficiency by 5 to 10%. This is an indication that, without further improvement of the method, one should increase the number of planes in order to get smooth phase masks with a good conversion efficiency.

The convergence of the algorithm is represented in figure 3c, where 1 iteration stands for the 9 planes computations in ascending order of z_l. For presentation purpose, we have run the optimal simulation starting from the result of the unparametrized one, but this is not a general requirement. So, the first 90 iterations are dedicated to the unparameterized algorithm. We start with a Fourier diaphragm parameter $\eta = 20$, to successively release it to 16, 12, and finally 8, every 20 iterations. After this, 50 iterations perform the optimization according to (5) with $\alpha = 1/100$, using the Nelder–Mead method. From the first iteration, we observe a strong

tightening of the conversion efficiency distribution. Concerning execution time, 1 iteration of the unparameterized algorithm only takes 20 seconds against 20 minutes for the optimal algorithm, the simulation running on a personal computer with an AMD Ryzen 6 cores cpu. Regarding stability, when running the unparameterized algorithm for a longer time we observe some accidental behaviors with some decays of the global conversion efficiency. This problem is due to the loss of unitarity introduced by the Fourier filtering of high spatial frequencies, because of which $O(\varphi)$ has no reason to remain invariant moving from one plane to another. On the other hand, the optimal algorithm seems to bring stability and no such accidents have been observed, even if a slight non-unitarity remains. Moreover, because such Fourier filtering of the modes is not totally rigorous physically, we have verified afterwards the validity of our design with a different propagation method based on the computation of Rayleigh–Sommerfeld integral [15].The difference between both propagation methods on the mean conversion efficiency appears to be less than 0.1%.

Furthermore, figure 3d provides a closer view on the final distribution of the squared overlaps obtained with both algorithms. We observe a striking decrease of the standard deviation, by a factor 17.2 in favor of the optimal algorithm. Furthermore, we stress that the balance of the overlaps is not obtained at the expense of the overall convergence: indeed, the mean value of the squared overlaps is nearly the same for both algorithms, being of 75.2% for the unparameterized algorithm and of 76.7% for the optimal one.

Finally, we report a surprising point concerning the crosstalks between modes, defined by the squared overlaps between u_i and v_j when $i \neq j$. As both algorithms fail to convert about 25% of the energy from u_i to v_i, we could expect to see this energy reappearing in a significant proportion in crosstalks. However, this is not the case since the estimated worst crosstalks represent only -19.7 dB in the unparameterized case and -21.4 dB in the optimal one. A possible interpretation is that the uncontrolled energy might be distributed randomly among the huge number of modes that can pass through the system.

5 Conclusion

We presented a general algorithm to perform multimode conversion through an optical system composed of multiple phase masks separated by free propagations. We introduced some optimization parameters and demonstrated the possibility of strongly improving the convergence properties, notably regarding overlap balancing and stabilization of the overlaps growth in spite of disturbing non-unitarity, without requiring any additional phase resources. The optimization technique we used may not be the most effective but yet proved its feasibility with a large number of modes and reasonable computational resources.

This study opens many questions concerning the large number of tuning parameters to explore in such algorithms, like the order of computation of the planes, the distances between planes or the mode layouts that lead to simpler transformations, to name a few. Moreover, the possibility of conserving unitarity by constraining masks smoothness, preferably without increasing the phase resources, remains a very important problem from both numerical and experimental perspectives, that we hope to address in some future work.

Acknowledgements

The author thanks gratefully Marc Brunel and Marco Romanelli from Institut Foton in Rennes for fruitful discussions and careful reading of the present article.

References

[1] K Dholakia and T Čižmár. Shaping the future of manipulation. *Nature Photonics*, 5(6):335, 2011.

[2] F. O. Fahrbach, P. Simon, and A. Rohrbach. Microscopy with self reconstructing beams. *Nature Photonics*, 4(11):780–785, 2010.

[3] A. E. Willner, H. Huang, Y. Yan, Y. Ren, N. Ahmed, G. Xie, C. Bao, L. Li, Y. Cao, Z. Zhao, J. Wang, M. P. J. Lavery, M. Tur, S. Ramachandran, A. F. Molisch, N. Ashrafi, and S. Ashrafi. Optical communications using orbital angular momentum beams. *Adv. Opt. Photon.*, 7(1):66–106, Mar 2015.

[4] T. Y. Fan. Laser beam combining for high-power, high-radiance sources. *IEEE Journal of Selected Topics in Quantum Electronics*, 11(3):567–577, May 2005.

[5] Koji Sugioka and Ya Cheng. Ultrafast lasers—reliable tools for advanced materials processing. *Light: Science & Applications*, 3(4):e149, 2014.

[6] Albertas Žukauskas, Ieva Matulaitienė, Domas Paipulas, Gediminas Niaura, Mangirdas Malinauskas, and Roaldas Gadonas. Tuning the refractive index in 3d direct laser writing lithography: towards grin microoptics. *Laser & Photonics Reviews*, 9(6):706–712, 2015.

[7] Andrew Forbes, Angela Dudley, and Melanie McLaren. Creation and detection of optical modes with spatial light modulators. *Advances in Optics and Photonics*, 8(2):200–227, 2016.

[8] Olivier Ripoll, Ville Kettunen, and Hans Peter Herzig. Review of iterative fourier-transform algorithms for beam shaping applications. *Optical Engineering*, 43(11):2549–2549, 2004.

[9] R.W. Gerchberg and A Saxton W. O. A practical algorithm for the determination of phase from image and diffraction plane pictures. *Optik*, 35:237–250, 11 1971.

[10] Gavin Sinclair, Jonathan Leach, Pamela Jordan, Graham Gibson, Eric Yao, Zsolt John Laczik, Miles J Padgett, and Johannes Courtial. Interactive application in holographic optical tweezers of a multi-plane gerchberg-saxton algorithm for three-dimensional light shaping. *Optics Express*, 12(8):1665–1670, 2004.

[11] W. Minster Kunkel and James R. Leger. Gradient-index design for mode conversion of diffracting beams. *Opt. Express*, 24(12):13480–13488, Jun 2016.

[12] Jean-François Morizur, Lachlan Nicholls, Pu Jian, Seiji Armstrong, Nicolas Treps, Boris Hage, Magnus Hsu, Warwick Bowen, Jiri Janousek, and Hans-A. Bachor. Programmable unitary spatial mode manipulation. *J. Opt. Soc. Am. A*, 27(11):2524–2531, Nov 2010.

[13] Nicolas Fontaine, Roland Ryf, Haoshuo Chen, David Neilson, and Joel Carpenter. Design of high order mode-multiplexers using multiplane light conversion. In *ECOC*, Sep 2017.

[14] Joseph W Goodman. *Introduction to Fourier optics*. Roberts and Company Publishers, 2005.

[15] Fabin Shen and Anbo Wang. Fast-fourier-transform based numerical integration method for the rayleigh-sommerfeld diffraction formula. *Applied optics*, 45(6):1102–1110, 2006.